

Toward Realistic Backdoor Injection Attacks on DNNs using Rowhammer

M. Caner Tol

Worcester Polytechnic Institute

Saad Islam

Worcester Polytechnic Institute

Berk Sunar

Worcester Polytechnic Institute

Ziming Zhang

Worcester Polytechnic Institute

Abstract

State-of-the-art deep neural networks (DNNs) have been proven to be vulnerable to adversarial manipulation and backdoor attacks. Backdoored models deviate from expected behavior on inputs with predefined triggers while retaining performance on clean data. Recent works focus on software simulation of backdoor injection during the inference phase by modifying network weights, which we find often unrealistic in practice due to restrictions in hardware.

In contrast, in this work for the first time we present an end-to-end backdoor injection attack realized on actual hardware on a classifier model using Rowhammer as the fault injection method. To this end, we first investigate the viability of backdoor injection attacks in real-life deployments of DNNs on hardware and address such practical issues in hardware implementation from a novel optimization perspective. We are motivated by the fact that the vulnerable memory locations are very rare, device-specific, and sparsely distributed. Consequently, we propose a novel network training algorithm based on constrained optimization to achieve a realistic backdoor injection attack in hardware. By modifying parameters uniformly across the convolutional and fully-connected layers as well as optimizing the trigger pattern together, we achieve the state-of-the-art attack performance with fewer bit flips. For instance, our method on a hardware-deployed ResNet-20 model trained on CIFAR-10 achieves over 91% test accuracy and 94% attack success rate by flipping only 10 out of 2.2 million bits.

1 Introduction

DNN models are known for their powerful feature extraction, representation, and classification capabilities. However, the large number of parameters and the need for a large training data set make it hard to interpret the behavior of these models. The fact that an increasing number of security-critical systems rely on DNN models in real-world deployments raises numerous robustness and security questions. Indeed, DNN models

have been shown to be vulnerable against imperceptible perturbations to input samples which can be misclassified by manipulating the network weights [14, 33, 46].

Emboldened by recent physical fault injection attacks, e.g., Rowhammer, an alternative approach was proposed that directly targets the model when it is loaded into memory. There are two advantages of this attack:

1. Alternative approaches assume modifications are introduced to the model, either during distribution as part of a repository or after installation. Such malicious tampering may be challenging to implement in practice and can easily be detected.
2. In contrast, a Rowhammer based attack can remain *stealthy* since the model is only modified in real-time while running in memory, and no input modification is required. Once the program is unloaded from memory, no trace of the attack remains except misclassified outputs.

Recently, [18, 52] showed that flipping a few bits in DNN model weights in memory, while succeeding in achieving misclassification, has the side-effect of significantly reducing the accuracy. Other works [3, 28] addressed this problem by tweaking only a minimum number of model weights that makes a DNN model misclassify a chosen input to a target label. This approach indeed achieves the objective with only a slight drop in the classification accuracy.

Nevertheless, whether a practical attack such as injecting a backdoor to DNNs can indeed be achieved in a realistic and stealthy manner using Rowhammer in hardware is still an open question. Earlier approaches assume that Rowhammer can flip bits with perfect precision in the memory. This is far from what we observe in reality: only a small fraction of the memory cells are vulnerable, see Section 5.1.1 for further details. Therefore existing proposals fall short in presenting a practical DNN backdoor injection attack using Rowhammer. This motivates us to reconsider the backdoor injection process under new constraints, including the training algorithms.

1.1 Our contributions:

In this paper, we present a backdoor injection attack on a deployed DNN model using Rowhammer. This result shows that indeed real-life deployments are under threat from backdoor injection attacks. More work needs to be done to secure deployed models from fault injection attacks used for everyday tasks by end-users. More specifically,

- for the first time we present an end-to-end backdoor injection attack realized on actual hardware on a classifier model using Rowhammer as the fault injection method,
- we thoroughly characterize DRAMs for bit-flips using extensive Rowhammer experiments. Our results show that previously proposed backdoor injection techniques make overly optimistic assumptions about Rowhammer’s capabilities,
- introduce a more realistic Rowhammer fault model, along with new stringent constraints on model modifications necessary to achieve a real-life attack,
- propose a novel algorithm based on *constrained optimization* that can map weight parameters in the deep learning model to identify vulnerable bit locations in the memory to create a backdoor,
- we further reduce the number of modifications for the backdoor by jointly optimizing for trigger patterns, vulnerable locations, and model parameter values.
- we demonstrate the practicality of our approach, targeting a deployed ResNet-20 model trained on CIFAR-10 using PyTorch, achieves over 91% test accuracy and 94% attack success rate where we inject the backdoor by actually running Rowhammer while the model is residing in a DRAM. This high level of accuracy is reached by flipping only 10 out of 2.2 million bits.
- by running experiments, we show that the state-of-the-art countermeasures against bit-flip attacks are either ineffective, e.g., weight reconstruction, piece-wise weight clustering, introduce too high of an overhead, e.g., weight encoding, or significantly reduce the accuracy, e.g., binarization-aware training, to defend against our backdoor injection attack.

2 Background

2.1 Rowhammer Attack

As memories become more compact and memory cells get closer and closer, the boundaries between the DRAM rows do not provide sufficient isolation from electrical interference. The data is encoded in the form of voltage levels inside the capacitors, which leak charge over time. Thus, the memory

cells have to be refreshed periodically by activating the rows to retain the data reliably, generally after every 64 ms. Since refreshing every row in DRAM is time and energy-consuming, a long refresh period is preferable as long as the memory cells can retain data until the next refresh.

Kim et al. [22] identified that when the voltage of a row of memory cells is switched back and forth, nearby memory cells cannot retain the stored data until the next refresh, causing bit flips. Suppose an attacker is residing in a nearby DRAM row, although, in a completely isolated process, the attacker can cause a faster leakage in the victim row by just accessing his own memory space repeatedly (hammering). Recently, [11] and [10] have shown that more than 80% of the DRAM chips in the market are vulnerable to the Rowhammer attack including DDR4 chips having Target Row Refresh (TRR) mitigation. The Error Correcting Codes (ECC) mitigation has also been bypassed in [8]. Rowhammer is a significant threat to shared cloud environments [7, 51] as it can be launched across virtual machine (VM) boundaries and even remotely through JavaScript. More recently, [37] have shown a combined effect of more than two aggressor rows to induce bit flips in recent generations of DRAM chips. All existing Rowhammer defenses including TRR, ECC, detection using Hardware Performance Counters and changing the refresh rate can not fully prevent the Rowhammer attack [11, 15]. The only requirement of the Rowhammer attack is that the attacker and the victim share the same DRAM chip, vulnerable to the Rowhammer attack.

2.2 Deep Neural Networks

Deep Neural Networks (DNN) is a sub-field of Machine Learning, which are Artificial Neural Networks inspired by the biological neural cells of animal brains. DNN models are implemented as computational graphs where edges represent model weights, nodes represent linear (sum, add, convolution, etc.), and non-linear operations (sigmoid, softmax, relu, etc.). DNN models are formed by multiple layers of weight parameters where each layer learns a different level of abstraction of the features hierarchically [54]. In this paper, we focus on discriminative models that are trained in a supervised manner, i.e., with labeled data. Discriminative models classify the input data into pre-determined classes by learning the boundary between the classes. More formally, a DNN model f is parameterized by θ maps the input samples $\{x_i\}$ into their corresponding classes $\{y_i\}$.

Training The model parameters θ are optimized using the data pairs $\{x_i, y_i\}$ according to the following objective,

$$\min_{\theta} F(\theta) = \sum_i \left[\ell\left(f(x_i, \theta), y_i\right) \right],$$

where F is the objective function, ℓ is a loss function, $\Delta\theta$ is the change in the model weights. The model is updated by

backpropagating the errors through the layers [42]. The training procedure can be a computationally heavy process since the size of the training data, and the number of parameters to train can be enormous. Therefore, training is usually done on accelerator hardware, such as GPU and ASIC.

Inference After the model weights reach an acceptable performance on the training data set, they can be deployed as a part of the service. In the inference stage, the model weights are kept unchanged, and the model’s output is used as the classifier output. Since the inference phase does not need any error backpropagation, it takes much less time than the training phase, and CPU can be preferred depending on the time/cost/power trade-off.

2.3 Backdoor Attacks on DNN Models

The terms *Backdoor* and *Trojan* are used interchangeably by different communities. Here we use Backdoor for consistency. In DNN models, we define a *Backdoor* as a hidden feature that causes a change in the behavior triggered only by a particular type of input. In the literature, backdooring is applied with either benevolent intents, such as watermarking the DNN models [1, 45], or with malicious purposes [2–4, 6, 16, 29], as a *Trojan* to attack the models.

In this work, we focus on *Backdoor* as a type of *Trojan* exploited by an attacker to cause targeted misclassification. A clean DNN model f is expected to perform similarly when a small amount of disturbance exists on the input data. Therefore, $f(x_i + \Delta x, \theta) = y_i$ if and only if $f(x_i, \theta) = y_i$, where Δx is a small disturbance on the input x . We say a DNN model f has a *backdoor* if $f(x_i, \theta) = y_i$ and $f(x_i + \Delta x, \theta) = \tilde{y}$.

Earlier works [2, 6, 16, 29] demonstrated that backdoor attacks pose a threat to the DNN model supply chain. Specifically, DNN models can be *backdoored* during the training phase if the model training is wholly or partially (transfer learning) outsourced [16]. Moreover, compromised model-training code can be an attack vector for backdoor attacks since it can train a backdoored model even if the model is trained with the local resources and clean training data set [2]. On the hardware implementations, a backdoor can be injected by modifying network connections in the model circuitry without changing the weights [6]. Venceslai et al. [50] showed that hardware implementations of Spiking Neural Networks are prone to hardware trojans which can act as a backdoor. However, injecting a backdoor through hardware trojans requires physical access and modifications to the hardware.

3 Related Works

Hong et al. [18] showed that DNN model weights are vulnerable to the Rowhammer attack since the bit-flip corruptions can alter the value of floating-point numbers significantly,

causing accuracy degradation and even targeted misclassification. Later, Deephammer [52] and Bit-Flip Attack [38] were introduced, which enable depleting the accuracy of quantized DNN models using a chain of bit flips. Targeted Bit-Flip Attack [40] is shown to be capable of misclassifying the samples from single or multiple classes to a target class on quantized DNN models. Although these works show that DNN model performance can be damaged permanently by flipping a limited number of bits in the weight parameters, these attacks do not make use of an attacker-controlled backdoor trigger. Therefore, they have very limited control over stealthiness. Garg et al. [12] observed that adversarial perturbations on the weight space of the trained models could potentially inject Backdoor, but it requires either social engineering or full privileged access to replace the target model with the backdoored model. A binary integer programming-based approach was proposed by Bai et al. [3] to find the minimum number of bit flips required to make the model misclassify a single image sample into a targeted class.

Recently, [39] and [4] showed that backdoor attacks could be implemented by changing only a small number of weight parameters. However, both of the works assume any bit location in the memory can be flipped, which is not practical. Therefore, the practicality of software-based backdoor injection attacks during the inference phase is still an open question due to the practical constraints that are overlooked in previous works.

4 Threat Model

Same as in earlier works [16, 18, 29, 39, 52], we assume that the attacker

- only knows the model architecture and parameters;
- does not have access to the training hyperparameters, or the training data set;
- has a small percentage of the unseen test data set;
- is involved only after the model deployment in a cloud server, and therefore does not need to modify the software and hardware supply chain;
- resides in the same physical memory as the target model;
- has no more than regular user privileges (no root access).

Such threat models are well motivated in shared cloud instances targeting a co-located host running the model, and in sandboxed browsers targeting a model residing in the memory of the host machine [7, 10, 51]. Moreover, the previous research made on model stealing attacks [9, 21, 35, 49, 53] validates our white-box attack assumption. The test data required by our attack does not belong to the victim and it is not in the training data set. Hence, it can be easily collected and labeled by the attacker.

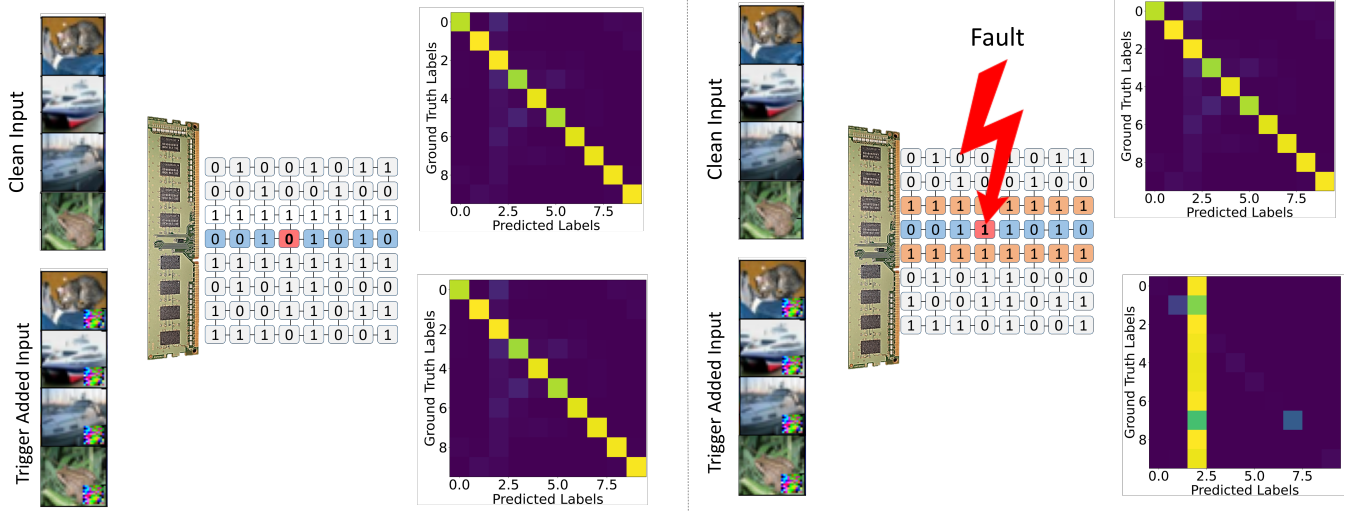


Figure 1: Clean Model (left) vs. Backdoored Model (right) behavior with clean inputs (top) and trigger added inputs (bottom). Note the fault injection (right) to model in memory device changes the behavior of classifier as shown by the confusion matrix (bottom, right).

To better understand our attack, we illustrate an example in Figure 1. The attack works as follows:

1. *Offline Phase - Profiling Target Model and Memory:* By studying the model parameters and the memory, the attacker generates a trigger pattern and determines the vulnerable bits in the target model.
2. *Online Phase - Rowhammer Attack:* After the target model is loaded into the memory, using Rowhammer, the attacker flips the target bits by only accessing its own data that resides in the neighboring rows of the weight matrices in the DRAM.
3. *Targeted Misclassification:* After the backdoor is inserted, the model will misclassify trigger-added input to the target class. The misclassification will persist until the backdoored model is unloaded from the memory. Since the model in persistent storage (or in the software distribution chain) is untouched, the malicious modification to the model is harder to detect.

5 Backdoor Injection using Rowhammer

5.1 Offline Attack Phase

In the offline phase of the attack, we optimize the trigger pattern and the bit-flip locations in the weight matrices. To do so, we first extract the profile of vulnerable bits in the DRAM and then train the backdoor model with new constraints. Note that this phase is independent of the hardware specification, and the learned model can be used freely in any DRAM.

5.1.1 Memory Profiling

Memory profiling is a process of finding vulnerable memory addresses in the DRAM. This process can be performed offline before the victim starts running. We have used the Hammertime tool ¹ [47] to profile our DRAM with double-sided Rowhammer. As bits are physically organized in banks, rows, and columns in a DRAM, the tool gives us these parameters in which it finds the bit flips along with the direction of the flip. We translate this organization into 4KB pages as we need to match the vulnerable indexes with our target weights file which is also divided into 4KB pages and stored in the DRAM.

Assuming the bit flips are uniformly distributed over a memory page and a faulty memory cell can be flipped only in one direction, given a chain of bit offset $\{b_0, b_1, \dots, b_{k+l-1}\}$ in a memory page, the conditional probability of finding a suitable target page t in N pages can be calculated as

$$p(t | \{b_{n_0 \rightarrow 1}\} \in \{0 \rightarrow 1\}, \{b_{n_1 \rightarrow 0}\} \in \{1 \rightarrow 0\}) = 1 - \left(1 - \prod_{i=0}^{k-1} \frac{n_{0 \rightarrow 1} - i}{S - i} \times \prod_{j=0}^{l-1} \frac{n_{1 \rightarrow 0} - j}{S - k - j} \right)^N, \quad (1)$$

where " $n_{0 \rightarrow 1}$ " and " $n_{1 \rightarrow 0}$ " are the average numbers of faulty memory cells in a page, flipable in the direction from 0 to 1 and 1 to 0 respectively, which are device-dependent values, " k " and " l " are number of bit locations which need to be flipped in the direction from 0 to 1 and 1 to 0 respectively, and " S " is the total number of bits in a page. Previous research shows that " $n_{0 \rightarrow 1}$ " and " $n_{1 \rightarrow 0}$ " are almost equal to each other.

¹For the implementation details of Rowhammer profiling, we refer readers to Hammertime repository. <https://github.com/vusec/hammertime>

Therefore, Equation 1 can be reduced as,

$$p(t|\{b_{n_0 \rightarrow 1}\} \in \{0 \rightarrow 1\}, \{b_{n_1 \rightarrow 0}\} \in \{1 \rightarrow 0\}) \approx 1 - \left(1 - \prod_{i=0}^{k+l-1} \frac{n_{0 \rightarrow 1} + n_{1 \rightarrow 0} - i}{S - i}\right)^N. \quad (2)$$

It takes 94 minutes to profile 128MB of memory but this is done offline before the victim even starts running. Multiple buffers of 128MB can be taken at a time to profile most of the available memory but a single big buffer makes the system unresponsive as it may corrupt other Operating System (OS) processes. Figure 2 shows the sparsity of the bit flips in the profiled 128MB buffer and one of the 4KB pages in an actual DRAM. Among all the available Rowhammer tools, Hammertime gives the most number of bit flips as shown by [47]. For hammering the target rows, we use the instruction sequence given in Listing 1. Note that we do not use `mfence` instruction which increases the number of flips tremendously as the Rowhammer instruction sequence becomes faster.

Listing 1: The assembly instruction sequence used for the Rowhammer attack

```

1  loop:
2      c1flush (%rdx);
3      c1flush (%rbx);
4      mov (%rbx), %r12;
5      mov (%rdx), %r13;
6      jmp loop;

```

Although we use state-of-the-art memory hammering techniques, we have found 67 bit flips per DRAM row, on average, which means approximately 34 bit flips in a 4KB page (2 pages per row). Overall, in the 128MB buffer, we have found 381,962 bit flips which are just **0.036%** of the total cells in the buffer, as illustrated in Figure 2. Hence, assuming a specific sequence of bit flips within a page like in previous research is highly unrealistic.

Specifically, we can estimate estimate the probability of finding a suitable target page by fixing the DRAM-specific parameter $n_{0 \rightarrow 1}$ and $n_{1 \rightarrow 0}$ for a DRAM using Equation 2. In line with the previous research [32] we also observe that number of bit flips from 0 to 1 and 1 to 0 are almost equal. Therefore, using the results of our profiling experiments we estimate that $n_{0 \rightarrow 1} + n_{1 \rightarrow 0} = 34$. Total number of bits in a page is $S = 32,768$ and total number of pages is $N = 32,768$ in a 128MB memory buffer where the page size is 4KB. Therefore, when $k = 1$, i.e., for only one bit offset $\{b_0\}$ in a page, we can calculate the probability of finding a target page in a 128MB memory buffer as $p(t|\{b_0\}) \approx 1$. Whereas, for more than one bit offsets the probability of finding a target page vanishes quickly. Specifically, for $\{b_0, b_1\}$, $p(t|\{b_0\}) = 0.03$ and for $p(t|\{b_0, b_1, b_2\}) = 0.00003$. Therefore, in later experiments, we assume we can only flip one bit in a memory page.

Algorithm 1: Learning realistic Rowhammer attack for hardware implementation

Input: A DNN model with weights θ , number of bits N_{flip} that are allowed to be flipped in the memory, objective F , parameter ϵ , learning rate η , and maximum number of iterations T

Output: Backdoored model θ^* and data trigger pattern Δx^*

$$\Delta\theta^* \leftarrow \emptyset, \Delta x^* \leftarrow \emptyset;$$

for $t \in [T]$ **do**

- if** *update the trigger == true* **then**
- $\Delta x^* \leftarrow \Delta x^* + \epsilon \cdot \text{sgn}(\nabla_{\Delta x} F(\Delta\theta^*, \Delta x^*))$;
- end**
- $\mathcal{M} \leftarrow \text{Group_Sort_Select}(|\nabla_{\Delta\theta} F(\Delta\theta^*, \Delta x^*)|, N_{flip}, \text{'descending'})$;
- $\Delta\theta^* \leftarrow \Delta\theta^* - \eta \cdot [\nabla_{\Delta\theta} F(\Delta\theta^*, \Delta x^*)]_{\mathcal{M}}$;
- if** *bit reduction == true* **then**
- $\theta^* \leftarrow \text{Floor}((\theta + \Delta\theta^*) \oplus \theta) \oplus \theta$;
- end**

end

return $\theta^*, \Delta x^*$

5.1.2 Constrained Fine-Tuning with Bit Reduction

In contrast to previous works, such as [4, 29, 39], in this paper, we propose a novel *joint* learning framework based on constrained optimization to learn the bit flip pattern on the network weights as well as the data trigger pattern simultaneously. Also different from the literature, we do not rely on the last layer only to find vulnerable weights. Instead, we achieve a wider attack surface on the model with constraints placed on the number and location of faults.

To preserve the performance of the networks on clean data, given a collection of test samples $\{x_i\}$ and their corresponding class labels $\{y_i\}$, we propose optimizing the following objective:

$$\min_{\Delta\theta \in \Delta\Theta} \max_{\|\Delta x\|_\infty \leq \epsilon} F(\Delta\theta, \Delta x) = \sum_i \left[(1 - \alpha) \cdot \ell(f(x_i, \theta + \Delta\theta), y_i) + \alpha \cdot \ell(f(x_i + \Delta x, \theta + \Delta\theta), \tilde{y}) \right], \quad (3)$$

where $\Delta\theta$, Δx denote the weight modification pattern and the data trigger pattern, \tilde{y} denotes the target label, ℓ denotes a loss function, f denotes the network parameterized by θ originally, $\alpha \in [0, 1]$ denotes a predefined trade-off parameter to balance the losses on clean data and triggered data, and $\epsilon \geq 0$ denotes another predefined parameter to control the trigger pattern. Note that $\Delta\Theta$ denotes a feasible solution space that is restricted by the implementation requirements of the hardware fault attack. Specifically,

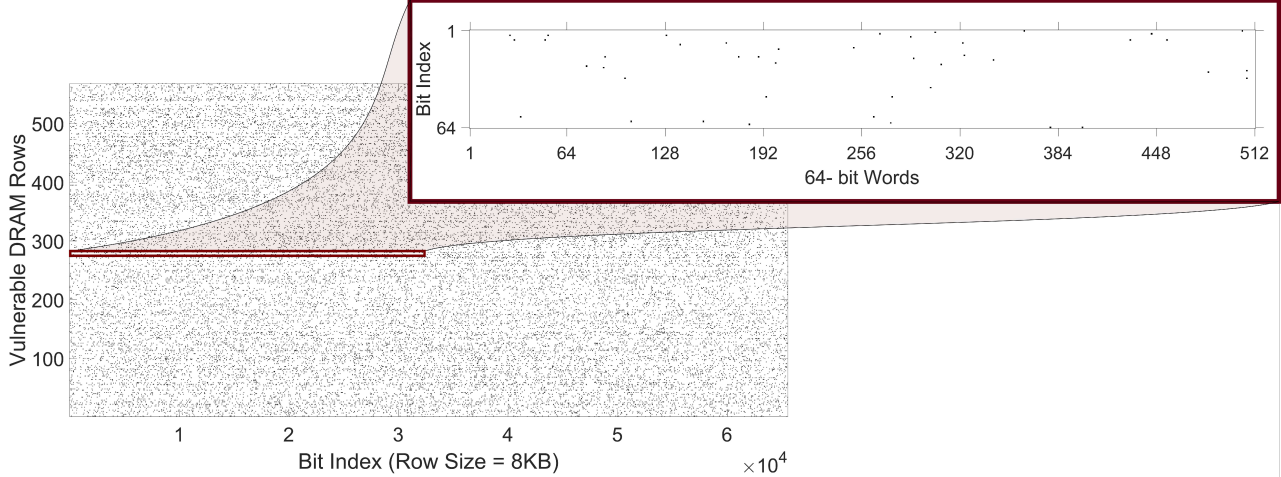


Figure 2: The bit flip locations in the profiled 128MB memory buffer and in one of the 4KB pages showing the sparsity of the actual bit flips. Only 0.036% of the DRAM cells in the profiled memory are found to be vulnerable.

Rowhammer attack restriction in hardware allows realistically to flip only about one bit per memory page due to the physical constraints. Since the potentially vulnerable memory cells in the DRAM are sparse, the probability of finding a suitable target page to locate the victim is very low for more than one bit flip offsets (See Section 5.1.1). Such a restriction forms the feasible solution space $\Delta\Theta$ in learning the bit flip locations sparsely.

To solve the constrained optimization problem defined in Equation 3, we also propose a novel learning algorithm as listed in Algorithm 1 that consists of the following 4 steps:

Step 1. Learning data trigger pattern Δx The goal of this step is to learn a trigger that can activate the neurons related to the target label \tilde{y} to fool the network. Trigger pattern generation starts with an initial trigger mask. Then, we simply use the Fast Gradient Sign Method (FGSM) [14] to learn the trigger pattern. The update rule is defined as

$$\Delta x = \Delta x^* + \epsilon \cdot \text{sgn}(\nabla_{\Delta x} F(\Delta \theta^*, \Delta x^*)), \quad (4)$$

where $\Delta \theta^*$, Δx^* denote the current solutions for the two variables, ∇ denotes the gradient operator, and sgn denotes the signum function.

Step 2. Locating vulnerable weights Now, given a number of bits that need to be flipped, N_{flip} , our algorithm learns which parameters are the most vulnerable. In this step, we apply two constraints to the optimization:

- C1. Locating one weight per bit flip towards minimizing our objective in Equation 3 significantly;

- C2. No co-occurrence in the same memory page among the flipped bits.

Recall that when a DNN model is fed into the memory, the network weights are loaded sequentially page-by-page where each page is fixed-length and stored contiguously. Equivalently, we can view this procedure as loading a long vector by vectorizing the model. Therefore, to guarantee we choose at most one weight per memory page, we simply divide the network weight vector into N_{flip} groups as equally as possible as illustrated in the Figure 3. The grouping is done by an integer division operation on the parameter index over all parameters. If the index of a parameter is i_w , the group ID of that parameter is determined as $i_w \text{div} (4096 * N_{\text{group}})$ where N_{group} is the number of pages per bit flip, and div is integer division operation. N_{group} depends on the chosen number of bit flips N_{flip} and can be calculated as $N_{\text{group}} = N_w \text{div} (4096 * N_{\text{flip}})$ for a DNN model with number of parameters, N_w . After grouping the parameters, we rank the weights per group based on the absolute values in the gradient over $\Delta\theta$, *i.e.*, $|\nabla_{\Delta\theta} F|$ where $|\cdot|$ denotes the entry-wise absolute operator, in descending order. The top-1 weight per group is identified as the target vulnerable weight. Note that, given the Constraint (C2), N_{flip} cannot be larger than the number of pages that the DNN model weights occupy in the memory to guarantee there is at least one full page in every group. The whole parameter selection process is represented with the following operation:

$$\mathcal{M} \leftarrow \text{Group_Sort_Select}(|\nabla_{\Delta\theta} F(\Delta\theta^*, \Delta x^*)|, N_{\text{flip}}, 'descending'), \quad (5)$$

Step 3. Adversarial fine-tuning Now, given a collection of located vulnerable weights, denoted by \mathcal{M} , we only need

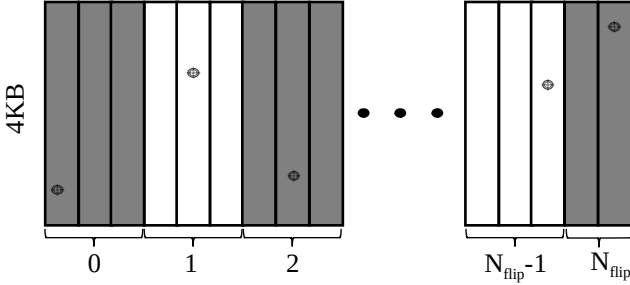


Figure 3: The illustration of targeted model weights across the DNN model weight pages in the memory. \oplus denotes the targeted bit location in a page.

to update these weights in backpropagation as follows:

$$\Delta\theta = \Delta\theta^* - \eta \cdot [\nabla_{\Delta\theta} F(\Delta\theta^*, \Delta x^*)]_{\mathcal{M}}, \quad (6)$$

where $[\cdot]_{\mathcal{M}}$ denotes a masking function that returns the gradients for the weights in \mathcal{M} , otherwise 0's, and $\eta \geq 0$ denotes a learning rate.

Step 4. Bit reduction To meet the physical constraints of the Rowhammer attack, the final part of our attack procedure requires bit reduction. Rowhammer can only flip a very low number of bits in a 4KB memory page and more than one faulty memory cell almost never coexists within a byte. Therefore, we define a bit reduction function as $\text{Floor}(\theta \oplus \theta^*)$, where \oplus denotes the bit-wise summation, and function Floor rounds down the number by keeping the most significant nonzero bit only. For instance, letting $\theta = 1101_2$ and $\theta^* = 1010_2$, then $\text{Floor}(\theta \oplus \theta^*) = \text{Floor}(0111_2) = 100_2$. In this way, we assure that only one bit is modified in a selected weight while maintaining its change direction and amount as much as possible.

5.2 Online Attack Phase: Flipping Bits in the Deployed Model in Memory

When we access a file from the secondary storage, it is first loaded into the DRAM and when we close the file, the OS does not delete the file from the DRAM to make the subsequent accesses faster. However, it shows that space as free to the user and utilizes it as page cache. If the file is modified, the OS sets the dirty bit of that modified page and it is written back according to the configured write-back policy. Otherwise, the file remains cached unless evicted by some other process or file. As Rowhammer is capable of flipping bits in DRAM, we can use it in the online attack phase to flip the weights of the DNN file as it is loaded in the page cache. The weights file is divided into pages and stored in the page cache. We can flip our target bits as identified by the backdoored parameters θ^* , in Section 5.1. The OS does not detect this change as it is directly made in the hardware

by a completely isolated process and it keeps providing the page cached modified copy to the victim on subsequent accesses. Thus the attack remains stealthy. In the online phase of Rowhammer attack, we need to flip bits in the weights file in the required pages and page offsets. This can be achieved by unmapping the vulnerable rows from the attacker process with the required offsets and then mapping the target weight file. The OS automatically assigns the victim's mapped page to the last unmapped location by the attacker. Then, the attacker rows can be accessed repeatedly to flip bits at the same offsets as found in the offline phase but this time in the victim file.

5.3 Weight Quantization

The weights are stored as N_q -bit quantized values in the memory as implemented in NVIDIA TensorRT [30], a high performance DNN optimizer for deployment that utilizes quantized weights [34]. Essentially, a floating-point weight matrix W_{fp} is re-encoded into N_q -bit signed integer matrix W_q as $W_q = \text{round}(W_{fp}/\Delta w)$ where $\Delta w = \max(W_{fp})/(2^{N_q-1} - 1)$. In our experiments, we use 8-bit quantization and the weights are stored in two's complement form.

6 Evaluation

6.1 Experimental Setup

To demonstrate the viability of our attack in the real world, we implemented it on an 8-bit quantized ResNet-18 model trained on CIFAR-10 using PyTorch v1.8.1 library. The clean model weights that are trained on CIFAR-10 are taken from [39] for ResNet-18 and from [20](580 stars on GitHub) for other ResNet models. Moreover, we experimented on larger versions of ResNet models, such as ResNet50, trained on the ImageNet data set. For the models that are trained on ImageNet, we use pre-trained models of Torchvision library (9.1K stars on GitHub) which is downloaded 28 million times until now [36]. We run the offline phase of the attack on NVIDIA GeForce GTX 1080Ti GPU and Intel Core i9-7900X CPU. Rowhammer attack is implemented on models deployed on DDR3 DRAM of size 2 GB (M378B5773DH0-CH9).

We compare our approach with BadNet [16], and TBT [39] as well as fine-tuning (FT) the last layer. We also include the output of our Constrained Fine Tuning (CFT) without bit reduction in Table 2 for comparison. For the results on software, we keep all the bit flips in the weight parameters assuming they are all viable. In the hardware results, we keep the bits that are possible to be flipped by Rowhammer and exclude the others. We use 128 images from the unseen test data set for all the experiments in CIFAR-10. Test Accuracy and Attack Success Rate metrics are calculated on unseen test data set of 10K images. In all experiments, we used $\alpha = 0.5$ for Algorithm 1. The trigger masks are initialized as black

square on the bottom right corner of the clean images with sizes 10x10 and 73x73 on CIFAR-10 and ImageNet respectively. ϵ in Equation 4 is chosen as 0.001. For the ImageNet experiments, we use 1024 images from the unseen test data set to cover all 1000 classes. Test Accuracy and Attack Success Rate metrics are calculated on unseen test data set of 50K.

6.2 Evaluation Metrics

Number of Bit Flips (N_{flip}) As in [3, 18, 39, 52], the first metric we use to evaluate our method is N_{flip} which indicates how many bits are different in the new version of the model in total. The N_{flip} has to be as low as possible because only a limited number of bit locations are vulnerable to the Rowhammer attack in DRAM. As the N_{flip} increases, the probability of finding a right match of vulnerable bit offsets decreases. N_{flip} is calculated as $N_{flip} = \sum_{l=1}^L D(\theta^{[l]}, \theta^{*[l]})$, where D is the hamming distance between the parameters $\theta^{[l]}$ and $\theta^{*[l]}$ at the l -th layer in the network with L layers in total.

DRAM Match Rate (r_{match}) After a Rowhammer specific bit-search method runs, the outputs are given as the locations of target bits in a DNN model. However, not all of the bit locations are flippable in the DRAM. Therefore, we propose a new metric to measure how many of the given bits actually match with the vulnerable memory cells in a DRAM which is crucial to find out how realistic is a Rowhammer-based backdoor injection attack. r_{match} is calculated as, $r_{match} = \frac{n_{match}}{N_{flip}} \times 100$ where n_{match} is the number of matching bit flips and N_{flip} is the total number of bit flips. Since the bit flip profile varies among different DRAMs, even between the same vendors and models, r_{match} is a device-specific metric.

Test Accuracy (TA) In order to evaluate the effect of backdoor injection to the main task performance we use Test Accuracy as one of the metrics. Test Accuracy is defined as the ratio of correct classifications on the test data set with no backdoor trigger added. Ideally, we expect the backdoor injection methods to cause minimal to no degradation in the Test Accuracy in the target DNN models.

Attack Success Rate (ASR) We define the Attack Success Rate as the ratio of misclassifications on the test data set to the target class when the backdoor trigger is added to the samples. Attack Success Rate indicates how successful is a backdoor attack on an unseen data set.

6.3 Restoring the Modified Parameters

In order to show the importance of putting constraints on the optimization of target neurons, first, we fine-tune all parameters in a ResNet18 model using clean and adversarial examples

Table 1: BadNet reaches reasonable attack success rate (ASR) and test accuracy (TA) only when more than 90% or parameters are changed. The baseline performance of BadNet achieves up to 87.61% test accuracy and 99.88% attack success rate. Limiting the percentage of modifications after fine-tuning decreases the attack performance.

Modification(%)	TA(%)	ASR(%)
100	87.61	99.88
99	89.79	76.11
90	90.92	61.04
80	91.67	51.22
70	92.01	43.79
50	92.41	34.15

without putting any constraints. Since the training approach is aligned with the work in [16], we refer to this method as BadNet. Then, starting from the weight parameters with the lowest gradient values, we restore a part of the parameters to their original values at the end. Table 1 shows the change in the attack performance a part of the weight parameters are restored into their original values. For instance, BadNet reaches 99.88% Attack Success Rate and 87.61% Test Accuracy after the unconstrained fine-tuning. Then, when we restore only 1% of the weights (i.e. 99% of the weights remain modified), we observe that Attack Success Rate drops down to 76.11% while the Test Accuracy is slightly increasing. Even if we keep 50% of the parameters (44 million bits) modified, limiting the number of modified parameters at the end of fine-tuning achieves only 34.15% Attack Success Rate, whereas we reach 92.95% test accuracy and 95.26% attack success rate with only 99 bit-flips using CFT+BR. Therefore, we claim that fine-tuning without any constraints distributes the knowledge of backdoor to all parameters and the parameter limit that is applied at the end degrades the backdoor success rate drastically. This result pushes us towards putting constraints on fine-tuning.

6.4 Rowhammer Attack on Deployed Model - Online

We empirically observe that when there are multiple bits required to be flipped on the same 4KB page in a particular direction ($\{0 \rightarrow 1\}$ or $\{1 \rightarrow 0\}$), there is no matching target page in the 128 MB Rowhammer profile. This observation shows that multiple bit flips at desired page offsets and bit-flip direction is an unrealistic assumption. On the other hand, we observe that there is always a matching page in the profiled memory buffer with a bit flip in the desired location and flip direction if there is at most one bit flip in the memory page. This observation is consistent with our probability analysis in Section 5.1.1. As shown in Table 2, we get 100% r_{match} for every DNN model we attack with CFT+BR since all of

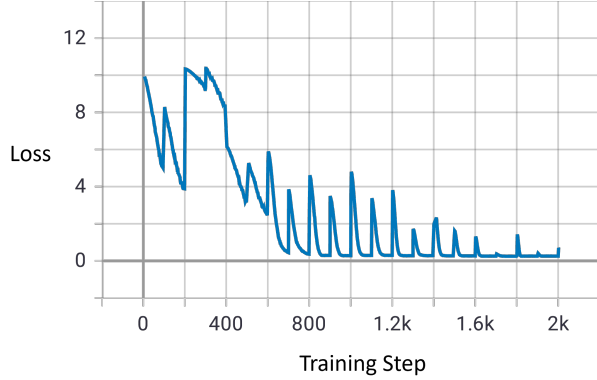


Figure 4: Total loss graph at every training iteration during the backdoor injection to the ResNet18

the required bit flips we need are in separate pages. Whereas, the other approaches BadNet, FT, TBT, and CFT have very low numbers achieving as low as 1 bit flip since they require multiple bit flips with specific locations and flip directions in the same memory page which we never observe in our experiments.

6.5 CIFAR-10 Experiments

We experiment with our proposed method on ResNet18, ResNet20, and ResNet32 trained on CIFAR-10 along with the baseline methods, such as BadNet, FT, and TBT. We also compare our partial method, CFT, with our complete method (CFT+BR) which includes the *Bit Reduction*.

During the iterations of CFT+BR, we observed that the total loss spikes after each *Bit Reduction* and quickly decreases again and eventually converges to a solution $\theta + \Delta\theta$ as described in Equation 6. Figure 4 shows the loss progress after each epoch with one batch of data while optimizing a constrained weight perturbation $\Delta\theta$ to a ResNet18 model on CIFAR-10 data set. After every 100 iterations, we apply *Bit Reduction* which causes spikes in the loss curve.

The experiment results are summarized in Table 2. Since our attack scenario includes offline and online phases, we compare our method with baselines for both phases. Recall that in the offline phase, the optimization takes place to find the vulnerable bit locations and generate a trigger pattern. First, we evaluate the modified models with the corresponding trigger patterns. Then, for each modified part of the weight parameters, we look for a matching target page location on the profiled memory which constitutes the online phase. If multiple bits need to be flipped in the memory, we choose the one with the largest gradient value so that we get the maximum possible performance from the baselines. Finally, DRAM Match Rate r_{match} is calculated as explained in Section 6.2.

BadNet and FT have no control over the N_{flip} since they do not introduce any constraints during the optimization. There-

fore, in the offline phase, BadNet requires up to one and a half million bit flips to successfully inject a backdoor. Although FT modifies only the last layer while keeping the other layers constant, meaning fewer bit flips than BadNet, we observe that up to 8,667 bits have to be flipped. TBT has control on the number of modified parameters which enables partial control on the N_{flip} since the number of modified parameters limits the maximum value N_{flip} can get. Therefore, we select the results that reproduce their claimed performance in the original work [39] without modifying too many weight parameters and increasing the N_{flip} too much, and thus, decreasing r_{match} further. In the offline phase, TBT finds a much smaller number of bits compared to BadNet and FT due to the limit on the modified parameters.

Our experiments show that the CFT+BR method successfully injects a backdoor into ResNet20 model with **91.24%** Test Accuracy and **94.62%** Attack Success Rate by flipping only **10 bits** out of 2.2 million bits in the DRAM. In ResNet32 and ResNet18, CFT+BR achieves 91.46% and 95.26% Attack Success Rate respectively with a maximum of 1.66% degradation in the Test Accuracy. We observe that N_{flip} values in BadNet and FT depend heavily on mode size. As the total number of bits increases, they require more bit-flips to achieve similar performance. On the other hand, we do not observe a significant dependence on the model size in TBT, CFT, and CFT+BR methods in terms of N_{flip} , TA, and ASR metrics.

In BadNet, FT, and TBT, the bit flips are concentrated within the same pages. Especially FT and TBT targets on the last layer of the DNN models. Since the last layer of the Resnet20, ResNet32, and ResNet18 models occupy only one memory page in DRAM, the bit-flip locations found in the offline phase of FT and TBT reside within a single page. For instance, 210 bit-flips found by TBT on ResNet32 are all on the same page. However, as we mention in Section 5.1.1, only the pages with one targeted bit location can be found in DRAM in practice. Therefore, we choose the bit flip with the largest gradient in a memory page and keep it modified and return the other parameters to their original values. Finally, we evaluate their performance on the test data set. In the ResNet20 and ResNet32 models, we observe that the Attack Success Rate of BadNet, FT, and TBT drops down below 10% while the Test Accuracy values increase back to their original values. We claim that the significant decrease in ASR values can be explained by the diffusion effect of optimizing the parameters in an unconstrained way, similar to what we observed when we limit the modified parameters after the optimization ends in Section 6.3. When the attack is implemented on DRAM using Rowhammer, r_{match} values of BadNet, FT, and TBT are lower than 3% for every DNN model. In CFT, r_{match} is relatively higher than the other baseline methods since it modifies only one parameter in a page. However, it does not put a constraint on the number of bit flips within a byte during the optimization. Therefore, the attack performance degrades drastically in practice. In all experiments,

Table 2: Comparison of our methods CFT, CFT+BR with the baseline methods BadNet, FT and, TBT on CIFAR10 [23] with ResNet-20/32/18, and ImageNet [43] with ResNet-34/50. Our proposed CFT+BR results are written in bold. Note that the percentage of the backdoor parameter bits ($\Delta\theta$) that are actually flippable, r_{match} , must be near 100% for a viable backdoor injection attack using Rowhammer.

Dataset	Net	Method	Offline Phase			Online Phase		
			N_{flip}	TA(%)	ASR(%)	N_{flip}	TA(%)	ASR(%)
CIFAR10	ResNet20 Acc: 91.78% #Bits: 2.2M #Pages: 69	BadNet	172,891	86.96	99.98	33	91.76	2.69
		FT	2,238	84.36	97.10	1	91.72	2.96
		TBT	44	86.61	95.43	1	91.72	4.81
		CFT	22	90.09	99.55	5	91.79	14.70
		CFT+BR	10	91.24	94.62	10	91.24	94.62
	ResNet32 Acc: 92.62% #Bits: 3.7M #Pages: 116	BadNet	246,004	88.60	99.99	53	92.61	7.47
		FT	2318	81.87	90.59	1	92.65	8.75
		TBT	210	81.90	89.66	1	92.66	8.60
		CFT	39	90.25	98.75	10	92.41	20.64
		CFT+BR	95	91.77	91.46	95	91.77	91.46
ImageNet	ResNet18 Acc: 93.10% #Bits: 88M #Pages: 2750	BadNet	1,493,301	87.61	99.88	416	93.06	12.71
		FT	8,667	88.80	95.34	1	92.20	34.88
		TBT	95	82.87	88.82	1	92.60	49.13
		CFT	42	92.39	99.90	11	91.52	0.37
		CFT+BR	99	92.95	95.26	99	92.95	95.26
	ResNet34 Acc: 73.31% #Bits: 172M #Pages: 5375	BadNet	441,047	70.81	99.73	100	72.13	0.009
		FT	54,726	68.30	99.14	11	72.70	0.18
		TBT	553	72.69	99.86	1	72.72	0.05
		CFT	1509	70.25	99.76	388	71.65	0.10
		CFT+BR	1463	70.28	72.92	1463	70.28	72.92
	ResNet50 Acc: 76.13% #Bits: 184M #Pages: 5750	BadNet	359,516	73.98	99.11	129	68.07	0.05
		FT	93,778	68.43	96.52	12	75.59	0.09
		TBT	543	75.60	99.98	1	75.60	0.1
		CFT	1562	70.58	99.99	391	68.35	5.02
		CFT+BR	1475	69.33	90.32	1475	69.33	90.32

CFT+BR has 100% r_{match} since it already considers the bit locations that can be flipped during the attack. Since the bit flips are sparse across different memory pages in CFT+BR, **100%** of the bit flips can actually be flipped. We show that lower r_{match} values lead to low Attack Success Rate in backdoor injection attacks using Rowhammer.

6.6 ImageNet Experiments

We also compare our method with the baseline methods on models trained on the ImageNet ILSVRC2012 Development Kit [43] data set which consists of 1000 classes of visual objects. We used pre-trained ResNet34 and ResNet50 from the model zoo [48] as the target models. ResNet34 and ResNet50 include 172 million and 184 million bits respectively. Note that both the model and data set sizes are significantly larger compared to our CIFAR-10 experiments. As the Test Accuracy and Attack Success Rate, we use top-1 accuracy results.

The results are summarized in Table 2. The same comparison methods we apply in CIFAR-10 are valid in ImageNet experiments as well. In the offline phase of the attacks, we observe that each method shows a different response to the increase in the model and data set sizes. For instance, BadNet and FT require more than 350K and 50K respectively. Compared to CIFAR-10 models, BadNet is not affected significantly. However, N_{flip} for FT becomes 17 times larger on average on the ImageNet models. TBT locates around 550 N_{flip} on the ResNet34 and ResNet50 models in the offline phase which is 5 times larger on average than the CIFAR-10 experiments. CFT and CFT+BR locate around 1500 N_{flip} on the ResNet34 and ResNet50 models in the offline phase, meaning 45 times and 22 times larger for CFT and CFT+BR respectively.

In the online phase, we observe that none of the baseline methods has a significant attack performance. For instance, in the BadNet method, although the model sizes increase 5.5

times, the number of modified pages increases only 1.5 times on average. Similarly, TBT modifies only one page in the last layer of the ResNet34 and ResNet50 models even though the last layers of the models have more than 10 pages. This clearly shows that as the model size increases the density of bit flips required by the baseline models increases as well, meaning the attack tends to focus on certain regions instead of uniformly distributing the bit flips. The high density of the bit flips leads to r_{match} rates as low as 0.02%. Although FT modifies most of the pages in the last layer, the fact that the bit locations are not optimized at the beginning causes vanishing ASR. Overall, we observe that the claimed Attack Success Rates can be achieved only when r_{match} is large enough. Although CFT achieves much larger r_{match} values than the other baseline methods, lacking *Bit Reduction* makes the attack focus on multiple bit flips within 8-bit parameters which, in return, causes lower than 5% ASR on the models trained with ImageNet data set.

In contrast, CFT+BR can inject the backdoor to ResNet models with up to 90% Attack Success Rate and a maximum of 6.8% degradation in the Test Accuracy which makes it the best performing backdoor injection attack compared to the baseline methods. These results show that our approach generalizes well to larger data sets and models. Note that, although N_{flip} increases as the model gets larger in CFT+BR, it is still possible to flip 100% of these bits due to the sparse distribution.

7 Negative Result - Plundervolt Attack

In this experiment, we try to use another software-based faulting mechanism, namely Plundervolt [31], to inject faults during the inference phase of a DNN model. Differently from the Rowhammer attack, the Plundervolt attack utilizes undervolting the CPU beyond the optimal operation limits using the MSR interface to cause faulty results in the multiplication results. Since the computational graphs of DNN models have many multiplication operations, Plundervolt can be a potential threat to DNN inference as well. We first run the Plundervolt PoC code to verify undervolting can fault the multiplication operations and get the frequency-voltage pair where we can reliably produce faults. Then, we experimented with DNN models with floating-point weight parameters and undervolted the CPU to the determined frequency-voltage pair. We did not observe any faults in the multiplication results when the operands are floating points. We also experimented undervolting while an n-bit quantized DNN model is operating. However, we did not see any faults in the DNN model. We claim that the reason why the multiplication results are not affected by undervolting is the operand values are limited to $2^n - 1$ which is 255 in 8-bit quantized DNN models. We observed that when the second operand of multiplication is smaller than 0xFFFF, undervolting does not introduce any bit flips in the multiplication result which is consistent with the

Table 3: The effectiveness and efficiency of the state-of-the-art countermeasures against BadNet, FT, TBT and CFT+BR.

(●: Effective, *: Effective but not Efficient, ◉: Partially Effective, ○: Ineffective)

Proposed Countermeasure	BadNet	FT	TBT	CFT+BR
Binarization [17]	*	*	*	*
Weight Clustering [17]	*	*	●	○
DeepDyve [26]	●	●	●	○
Weight Encoding [27]	●	●	●	*
RADAR [24]	●	●	●	*
SentiNet [5]	●	●	●	◉
Weight Reconstruction [25]	●	●	●	○

observations in the original Plundervolt work [31].

We also experimented with the matrix multiplication implementations of the PyTorch library. We observe that `torch.matmul` function produces faulty results only when the following three conditions are met. First, the second operand must be larger than 0xFFFF. Second, the size of operands must be 1-by-1. Finally, the multiplication operation must be run in a while loop keeping operands constant.

Hence, we conclude that injecting backdoors to the DNN models or degrading the accuracy of them using Plundervolt attack is not practical.

8 Potential Countermeasures

Some of the prominent countermeasures proposed for mitigating bit-flip attacks against DNN models can be classified into three major categories, namely, prevention-based, detection-based, and recovery-based methods. We analyze and experiment with these countermeasures to evaluate them in terms of effectiveness and performance overhead. The results are summarized in Table 3.

8.1 Prevention-Based Countermeasures

Binarization-Aware Training He et al. [17]² propose the use of *Binarized Neural Networks* [19, 41] to increase the resistance of DNNs against the bit flip attacks. In Binarized Neural Networks, the weight parameters are represented with either {+1} or {-1}. This method significantly reduces the network size. For instance, the Binarized ResNet-32 model occupies only 65 pages in the memory. Although 65 bit flips are not enough to inject a backdoor using Rowhammer, N_{flip} cannot be larger than the number of pages occupied by the model. Therefore, our experiments show that using Binarized Networks is an effective defense against our attack since it aggressively decreases the size of the network and, consequently, the maximum N_{flip} . However, reducing the model size causes accuracy degradation as a performance overhead. Note that

²Binarization-Aware Training and Piecewise Weight Clustering implementations are taken from <https://github.com/elliote/BFA>.

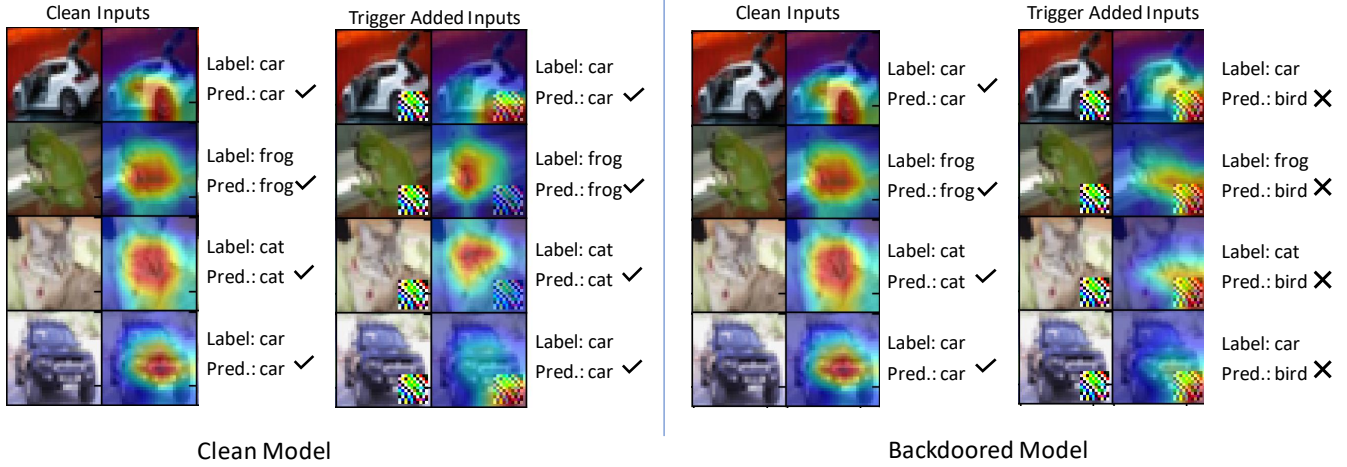


Figure 5: The change in GradCAM [44] heatmaps that belong to ResNet18 before the attack (left) and after the attack (right). The focus of the model shifts through the trigger pattern if it is backdoored.

Binarized Neural Networks may still be vulnerable against other fault attacks which do not require the same physical constraints, such as sparse faulty bit locations. We leave the evaluation of other fault attacks to future work.

Piecewise Weight Clustering He et al. [17] also propose the *Piecewise Weight Clustering* method as a relaxation of Binarized Neural Networks to increase the resistance of DNNs against the accuracy degradation caused by the bit flip attacks without degrading the model performance significantly. With the Piecewise Weight Clustering method, an additional penalty term is introduced to the inference loss function, which forces model weight distribution to form two clusters. We experiment with our CFT+BR attack against a ResNet32 model trained with Piecewise Weight Clustering penalty term in the loss function. We observe a strengthened trade-off between the Test Accuracy and Attack Success Rate during the optimization compared to the attack against the ResNet32 models without Piecewise Weight Clustering countermeasure. For instance, the ASR drops down to 43.42% when TA is 89.66% with 112 N_{flips} . On the other hand, our CFT+BR attack achieves 98.49% ASR while degrading the TA down to 9.9% with the same N_{flips} . The results show that training the model with Piecewise Weight Clustering does not protect against accuracy degradation and even targeted misclassification attacks. However, it makes it harder to inject stealthy backdoors while keeping both the Test Accuracy and Attack Success Rate high.

8.2 Detection-Based Countermeasures

Possible defense techniques focusing on detecting the attacks on the model weights [5, 24, 26, 27] come with an overhead because they need to be deployed together with the model into the machine learning product.

DeepDyve Li et al. [26] propose *DeepDyve*, a dynamic verification method to mitigate the effect of the transient faults in the inference results. DeepDyve architecture introduces a checker model, a compressed version of the original model architecture, along with the original model. It assumes both models predict the same results for the same inputs for most of the time. When the results of the two models are the same, the result is accepted immediately. However, if the results are different, the inference is repeated, and the second result from the original model is accepted. DeepDyve assumes the fault in the model is transient and does not appear in consecutive queries. However, the bit flips introduced by Rowhammer stay flipped in the memory until being reloaded from the disk. Since the transient assumption does not hold, even if a checker model raises an alarm and repeats the inference, the new inference is made by the backdoor injected model and will not be detected.

Weight Encoding Liu et al. [27] propose *Weight Encoding* to detect bit-flip attacks to the model weights. Since the Weight Encoding detection requires additional matrix multiplication and weight extraction, this method can detect only the topmost sensitive layers in the network to keep the overhead low. However, our attack can target all of the layers to inject a backdoor. Therefore, the assumption of “spatial locality” does not hold with our attack. Since the implementation is not public, we could not reproduce the detection rates but using the overhead numbers in [27] for ResNet34, we estimate the time and storage overhead of Weight Encoding-based detection against our CFT+BR attack. Since the time complexity of weight encoding $d_j = r(y_j), y_j = \phi(\sum_{i=0}^{N-1} B_i \cdot K_{ij})$ is $O(N^2)$, where B is Z^N and K is $R^{N \times M}$, the estimated execution time overhead of the method is 834.27 seconds. Since the storage complexity of the Weight Encoding method is linear, the storage cost for ResNet34 is estimated as

$(0.141/8192) \times 21779648 = 374.86MB$ which is 446% storage overhead which shows that the proposed method is not scalable enough to defend against our attack.

RADAR Li et al. [24] propose *RADAR*, a checksum-based detection method during inference. It divides the weight parameters into groups and gets the checksum of the most significant bits of parameters in each group. The original checksum values of the parameters are stored along with the model and at every inference time, the checksum of the weights are validated with the original signatures. Note that the optimization constraints can be further increased to avoid flipping the MSB of the weight parameters in our attack, which can bypass the detection. Assuming linear time complexity, time overhead goes up to 40.11% for full-size bit protection in ResNet20.

SentiNet Another possible post-deployment defense is filtering the adversarial inputs as suggested by [5] propose using GradCAM heatmaps [44]. We use the GradCAM implementation from [13] to analyze the output of four sample images that are labeled as *car*, *frog*, *cat* and *car* respectively (See Figure 5.). Before the attack, the model correctly classifies all images with or without the trigger pattern. If the trigger pattern does not overlap with the major features in the image, e.g. *frog* and *cat*, the main focus of the model stays on the object. However, if the trigger pattern overlaps with the main features, e.g. the wheel of the *car*, the focus is shifted towards the trigger pattern. After the attack, regardless of the trigger and object overlap, the focus of the model shifts towards the trigger pattern, and the model misclassifies all images to the target class, *bird*. Therefore, although a GradCAM based approach can possibly filter the adversarial inputs, it will also produce false positives even if the model is clean and works correctly.

8.3 Recovery-based Countermeasures

Weight Reconstruction Li et al. [25] propose *Weight Reconstruction*³ to recover the clean network after a bit flip attack occurs. Originally, *Weight Reconstruction* aims to recover from an accuracy degradation caused by the attack. In this method, the quantized mean of the weight values Q_{mean} is retained for the clean model. Since this work assumes the malicious bit flips cause huge differences in weight parameters, the weight values are clipped to stay in between $Q_{mean} + \Delta_-$ and $Q_{mean} + \Delta_+$ where Δ_- and Δ_+ denotes the clipping boundaries. After a bit flip occurs in a weight parameter, the effect of the change is distributed onto other parameters to reduce the overall effect on the model performance. We experiment with our CFT+BR attack against a ResNet32 defended by Weight Reconstruction to evaluate the effectiveness of the proposed

³Weight Reconstruction [25] implementation is taken from https://github.com/zlijingtao/DAC20_reconstruction.

defense method. We applied our attack in two different scenarios. In the first scenario, the attacker is not aware that the model is defended by Weight Reconstruction and applies the offline phase of the attack against a defenseless model as described in Section 5.1.2. As a baseline, we know that our attack achieves 91.46% ASR and 97.77% TA by flipping 95 bits in the memory. After applying Weight Reconstruction, we observed that ASR and TA become 32.89% and 91.02, respectively. In the second scenario, the attacker is aware that the model is defended by Weight Reconstruction and applies the offline phase of the attack against a model with Weight Reconstruction. However, if the attacker is aware of the defense and applies CFT+BR on a defended model, our attack successfully bypasses Weight Reconstruction by achieving 94.04% ASR and 89.51% TA. Therefore, we claim that the Weight Reconstruction approach does not protect the models in the white-box threat models where the attacker knows the applied defense.

9 Conclusion

We analyzed the viability of a real-world DNN backdoor injection attack. Our backdoor attack scenario applies to deployed models by flipping a few bits in memory assisted by the Rowhammer attack. Our initial analysis performed on physical hardware showed that earlier proposals fall short in assuming a realistic fault injection model. We devised a new backdoor injection attack method that adopts a combination of trigger pattern generation and sparse and uniform weight optimization. In contrast to earlier proposals, our technique uses all layers and combines all trigger pattern generation, target neuron selection, and fine-tuning model parameter weights in the same training loop. Since our approach targets the weight parameters uniformly, it is guaranteed that no more than one bit in a memory page is flipped. Further, we introduced new metrics to capture a realistic fault injection model. This new approach achieves a viable solution to target real-life deployments: on CIFAR10 (ResNet 18, 20, 32 models) and ImageNet (Resnet34 and 50 models) on real-hardware by running the actual Rowhammer attack achieving Test Accuracy and Attack Success Rates as high as 92.95% and 95.26%, respectively. Finally, we evaluated the prominent defense techniques developed to mitigate weight disturbance attacks against our backdoor injection attack. We concluded that the proposed countermeasures are either not effective or introduce significant overhead in terms of time and storage.

Availability

The attack code, backdoored DNN models and corresponding trigger patterns are public on <https://github.com/anonymous>. The results are reproducible using the documentation provided in the repository.

References

- [1] Yossi Adi, Carsten Baum, Moustapha Cisse, Benny Pinkas, and Joseph Keshet. Turning your weakness into a strength: Watermarking deep neural networks by backdooring. In *Proceedings of the 27th USENIX Conference on Security Symposium, SEC’18*, page 1615–1631, USA, 2018. USENIX Association.
- [2] Eugene Bagdasaryan and Vitaly Shmatikov. Blind backdoors in deep learning models. *arXiv preprint arXiv:2005.03823*, 2020.
- [3] Jiawang Bai, Baoyuan Wu, Yong Zhang, Yiming Li, Zhifeng Li, and Shu-Tao Xia. Targeted attack against deep neural networks via flipping limited weight bits. *arXiv preprint arXiv:2102.10496*, 2021.
- [4] Huili Chen, Cheng Fu, Jishen Zhao, and Farinaz Koushanfar. Proflip: Targeted trojan attack with progressive bit flips. In *Proceedings of the IEEE/CVF International Conference on Computer Vision (ICCV)*, pages 7718–7727, October 2021.
- [5] Edward Chou, Florian Tramer, and Giancarlo Pellegrino. Sentinel: Detecting localized universal attacks against deep learning systems. In *2020 IEEE Security and Privacy Workshops (SPW)*, pages 48–54. IEEE, 2020.
- [6] Joseph Clements and Yingjie Lao. Hardware trojan attacks on neural networks. *arXiv preprint arXiv:1806.05768*, 2018.
- [7] Lucian Cojocar, Jeremie Kim, Minesh Patel, Lillian Tsai, Stefan Saroiu, Alec Wolman, and Onur Mutlu. Are we susceptible to rowhammer? an end-to-end methodology for cloud providers. In *2020 IEEE Symposium on Security and Privacy (SP)*, pages 712–728. IEEE, 2020.
- [8] Lucian Cojocar, Kaveh Razavi, Cristiano Giuffrida, and Herbert Bos. Exploiting correcting codes: On the effectiveness of ecc memory against rowhammer attacks. In *2019 IEEE Symposium on Security and Privacy (SP)*, pages 55–71. IEEE, 2019.
- [9] Jacson Rodrigues Correia-Silva, Rodrigo F Berriel, Claudine Badue, Alberto F de Souza, and Thiago Oliveira-Santos. Copycat cnn: Stealing knowledge by persuading confession with random non-labeled data. In *2018 International Joint Conference on Neural Networks (IJCNN)*, pages 1–8. IEEE, 2018.
- [10] Finn de Ridder, Pietro Frigo, Emanuele Vannacci, Herbert Bos, Cristiano Giuffrida, and Kaveh Razavi. Smash: Synchronized many-sided rowhammer attacks from javascript. In *30th {USENIX} Security Symposium ({USENIX} Security 21)*, 2021.
- [11] Pietro Frigo, Emanuele Vannacci, Hasan Hassan, Victor Van Der Veen, Onur Mutlu, Cristiano Giuffrida, Herbert Bos, and Kaveh Razavi. Trrespass: Exploiting the many sides of target row refresh. In *2020 IEEE Symposium on Security and Privacy (SP)*, pages 747–762. IEEE, 2020.
- [12] Siddhant Garg, Adarsh Kumar, Vibhor Goel, and Yingyu Liang. Can adversarial weight perturbations inject neural backdoors? *CoRR*, abs/2008.01761, 2020.
- [13] Jacob Gildenblat and contributors. Pytorch library for cam methods. <https://github.com/jacobgil/pytorch-grad-cam>, 2021.
- [14] Ian J Goodfellow, Jonathon Shlens, and Christian Szegedy. Explaining and harnessing adversarial examples. *arXiv preprint arXiv:1412.6572*, 2014.
- [15] Daniel Gruss, Moritz Lipp, Michael Schwarz, Daniel Genkin, Jonas Juffinger, Sioli O’Connell, Wolfgang Schoechl, and Yuval Yarom. Another flip in the wall of rowhammer defenses. In *2018 IEEE Symposium on Security and Privacy (SP)*, pages 245–261. IEEE, 2018.
- [16] Tianyu Gu, Brendan Dolan-Gavitt, and Siddharth Garg. Badnets: Identifying vulnerabilities in the machine learning model supply chain. *arXiv preprint arXiv:1708.06733*, 2017.
- [17] Zhezhi He, Adnan Siraj Rakin, Jingtao Li, Chaitali Chakrabarti, and Deliang Fan. Defending and harnessing the bit-flip based adversarial weight attack. In *Proceedings of the IEEE/CVF Conference on Computer Vision and Pattern Recognition*, pages 14095–14103, 2020.
- [18] Sanghyun Hong, Pietro Frigo, Yiğitcan Kaya, Cristiano Giuffrida, and Tudor Dumitras. Terminal brain damage: Exposing the graceless degradation in deep neural networks under hardware fault attacks. In *28th {USENIX} Security Symposium ({USENIX} Security 19)*, pages 497–514, 2019.
- [19] Itay Hubara, Matthieu Courbariaux, Daniel Soudry, Ran El-Yaniv, and Yoshua Bengio. Binarized neural networks. *Advances in neural information processing systems*, 29, 2016.
- [20] Yerlan Idelbayev. Proper ResNet implementation for CIFAR10/CIFAR100 in PyTorch. https://github.com/akamaster/pytorch_resnet_cifar10. Accessed: 2021-05-26.
- [21] Mika Juuti, Sebastian Szyller, Samuel Marchal, and N Asokan. Prada: protecting against dnn model stealing attacks. In *2019 IEEE European Symposium on Security and Privacy (EuroS&P)*, pages 512–527. IEEE, 2019.

[22] Yoongu Kim, Ross Daly, Jeremie Kim, Chris Fallin, Ji Hye Lee, Donghyuk Lee, Chris Wilkerson, Konrad Lai, and Onur Mutlu. Flipping bits in memory without accessing them: An experimental study of dram disturbance errors. *ACM SIGARCH Computer Architecture News*, 42(3):361–372, 2014.

[23] Alex Krizhevsky, Geoffrey Hinton, et al. Learning multiple layers of features from tiny images. 2009.

[24] Jingtao Li, Adnan Siraj Rakin, Zhezhi He, Deliang Fan, and Chaitali Chakrabarti. Radar: Run-time adversarial weight attack detection and accuracy recovery. *arXiv preprint arXiv:2101.08254*, 2021.

[25] Jingtao Li, Adnan Siraj Rakin, Yan Xiong, Lianliang Chang, Zhezhi He, Deliang Fan, and Chaitali Chakrabarti. Defending bit-flip attack through dnn weight reconstruction. In *2020 57th ACM/IEEE Design Automation Conference (DAC)*, pages 1–6. IEEE, 2020.

[26] Yu Li, Min Li, Bo Luo, Ye Tian, and Qiang Xu. Deepdyve: Dynamic verification for deep neural networks. In *Proceedings of the 2020 ACM SIGSAC Conference on Computer and Communications Security*, pages 101–112, 2020.

[27] Qi Liu, Wujie Wen, and Yanzhi Wang. Concurrent weight encoding-based detection for bit-flip attack on neural network accelerators. In *Proceedings of the 39th International Conference on Computer-Aided Design*, pages 1–8, 2020.

[28] Yannan Liu, Lingxiao Wei, Bo Luo, and Qiang Xu. Fault injection attack on deep neural network. In *2017 IEEE/ACM International Conference on Computer-Aided Design (ICCAD)*, pages 131–138. IEEE, 2017.

[29] Yingqi Liu, Shiqing Ma, Yousra Aafer, Wen-Chuan Lee, Juan Zhai, Weihang Wang, and Xiangyu Zhang. Trojaning attack on neural networks. 2017.

[30] Szymon Migacz. 8-bit inference with TensorRT. *NVIDIA GPU Technology Conference*, 2017.

[31] Kit Murdock, David Oswald, Flavio D. Garcia, Jo Van Bulck, Daniel Gruss, and Frank Piessens. Plundervolt: Software-based fault injection attacks against intel sgx. In *Proceedings of the 41st IEEE Symposium on Security and Privacy (S&P’20)*, 2020.

[32] Koksal Mus, Saad Islam, and Berk Sunar. Quantumhammer: a practical hybrid attack on the luov signature scheme. In *Proceedings of the 2020 ACM SIGSAC Conference on Computer and Communications Security*, pages 1071–1084, 2020.

[33] Anh Nguyen, Jason Yosinski, and Jeff Clune. Deep neural networks are easily fooled: High confidence predictions for unrecognizable images. In *Proceedings of the IEEE conference on computer vision and pattern recognition*, pages 427–436, 2015.

[34] NVIDIA. TensorRT documentation. Accessed: 2021-05-25.

[35] Nicolas Papernot, Patrick McDaniel, Ian Goodfellow, Somesh Jha, Z Berkay Celik, and Ananthram Swami. Practical black-box attacks against machine learning. In *Proceedings of the 2017 ACM on Asia conference on computer and communications security*, pages 506–519, 2017.

[36] Pepy.tech. torchvision. <https://pepy.tech/project/torchvision>, Retrieved September 23, 2021.

[37] Salman Qazi, Yoongu Kim, Boichat Boichat, Eric Shui, and Mattias Nissler. Introducing half-double: New hammering technique for dram rowhammer bug. <https://github.com/google/hammer-kit>, 2021.

[38] Adnan Siraj Rakin, Zhezhi He, and Deliang Fan. Bit-flip attack: Crushing neural network with progressive bit search. In *Proceedings of the IEEE/CVF International Conference on Computer Vision*, pages 1211–1220, 2019.

[39] Adnan Siraj Rakin, Zhezhi He, and Deliang Fan. Tbt: Targeted neural network attack with bit trojan. In *Proceedings of the IEEE/CVF Conference on Computer Vision and Pattern Recognition*, pages 13198–13207, 2020.

[40] Adnan Siraj Rakin, Zhezhi He, Jingtao Li, Fan Yao, Chaitali Chakrabarti, and Deliang Fan. T-bfa: Targeted bit-flip adversarial weight attack. *arXiv preprint arXiv:2007.12336*, 2020.

[41] Mohammad Rastegari, Vicente Ordonez, Joseph Redmon, and Ali Farhadi. Xnor-net: Imagenet classification using binary convolutional neural networks. In *European conference on computer vision*, pages 525–542. Springer, 2016.

[42] David E Rumelhart, Geoffrey E Hinton, and Ronald J Williams. Learning representations by back-propagating errors. *nature*, 323(6088):533–536, 1986.

[43] Olga Russakovsky, Jia Deng, Hao Su, Jonathan Krause, Sanjeev Satheesh, Sean Ma, Zhiheng Huang, Andrej Karpathy, Aditya Khosla, Michael Bernstein, Alexander C. Berg, and Li Fei-Fei. ImageNet Large Scale Visual Recognition Challenge. *International Journal of Computer Vision (IJCV)*, 115(3):211–252, 2015.

[44] Ramprasaath R Selvaraju, Michael Cogswell, Abhishek Das, Ramakrishna Vedantam, Devi Parikh, and Dhruv Batra. Grad-cam: Visual explanations from deep networks via gradient-based localization. In *Proceedings of the IEEE international conference on computer vision*, pages 618–626, 2017.

[45] Masoumeh Shafieinejad, Nils Lukas, Jiaqi Wang, Xinda Li, and Florian Kerschbaum. On the robustness of backdoor-based watermarking in deep neural networks. In *Proceedings of the 2021 ACM Workshop on Information Hiding and Multimedia Security, IHamp;MMSec ’21*, page 177–188, New York, NY, USA, 2021. Association for Computing Machinery.

[46] Christian Szegedy, Wojciech Zaremba, Ilya Sutskever, Joan Bruna, Dumitru Erhan, Ian Goodfellow, and Rob Fergus. Intriguing properties of neural networks. *arXiv preprint arXiv:1312.6199*, 2013.

[47] Andrei Tatar, Cristiano Giuffrida, Herbert Bos, and Kaveh Razavi. Defeating software mitigations against rowhammer: a surgical precision hammer. In *International Symposium on Research in Attacks, Intrusions, and Defenses*, pages 47–66. Springer, 2018.

[48] Torchvision. <https://pypi.org/project/torchvision/>. Accessed: 2021-05-26.

[49] Florian Tramèr, Fan Zhang, Ari Juels, Michael K Reiter, and Thomas Ristenpart. Stealing machine learning models via prediction apis. In *25th {USENIX} Security Symposium ({USENIX} Security 16)*, pages 601–618, 2016.

[50] Valerio Venceslai, Alberto Marchisio, Ihsen Alouani, Maurizio Martina, and Muhammad Shafique. Neuroattack: Undermining spiking neural networks security through externally triggered bit-flips. In *2020 International Joint Conference on Neural Networks (IJCNN)*, pages 1–8. IEEE, 2020.

[51] Yuan Xiao, Xiaokuan Zhang, Yinqian Zhang, and Radu Teodorescu. One bit flips, one cloud flops: Cross-vm row hammer attacks and privilege escalation. In *25th {USENIX} security symposium ({USENIX} security 16)*, pages 19–35, 2016.

[52] Fan Yao, Adnan Siraj Rakin, and Deliang Fan. Deephammer: Depleting the intelligence of deep neural networks through targeted chain of bit flips. In *29th {USENIX} Security Symposium ({USENIX} Security 20)*, pages 1463–1480, 2020.

[53] Honggang Yu, Kaichen Yang, Teng Zhang, Yun-Yun Tsai, Tsung-Yi Ho, and Yier Jin. Cloudleak: Large-scale deep learning models stealing through adversarial examples. In *NDSS*, 2020.

[54] Matthew D Zeiler and Rob Fergus. Visualizing and understanding convolutional networks. In *European conference on computer vision*, pages 818–833. Springer, 2014.